

Ketone-amine based suspensions for electrophoretic deposition of Al_2O_3 and ZrO_2

Guy Anné, Kim Vanmeensel, Bram Neirinck, Omer Van der Biest, Jef Vleugels*

Department of Metallurgy and Materials Engineering (MTM), K.U. Leuven, Kasteelpark Arenberg 44, B-3001, Heverlee, Belgium

Received 20 October 2005; received in revised form 10 January 2006; accepted 21 January 2006

Available online 20 March 2006

Abstract

Stable suspensions based on methylethylketone (MEK), *n*-butylamine and nitrocellulose were developed for the electrophoretic deposition (EPD) of Al_2O_3 and ZrO_2 powder. Deposits with a high green density, smooth surface and high deposition yield were obtained upon adding 10–15 vol.% *n*-butylamine in combination with 1 wt.% nitrocellulose. The influence of the reaction between MEK and *n*-butylamine, forming water and imines, on the electrophoretic deposition behaviour was investigated. Experimental results revealed that the zeta potential is not a straightforward indication of the stability of these suspensions, since the maximum absolute zeta potential did not correspond with a maximum suspension stability, due to the additional electrosteric stabilisation of the adsorbed charged nitrocellulose.

© 2006 Elsevier Ltd. All rights reserved.

Keywords: Suspensions; Shaping; Electrophoretic deposition; Al_2O_3 ; ZrO_2

1. Introduction

Colloidal processes have become very popular in processing ceramic materials because the defect sizes are smaller compared to dry pressing and because it allows a safe handling and manipulation of very fine and even nanometer sized powders. Among the different colloidal processing techniques, electrophoretic deposition is very promising because it is a fairly rapid, low cost process for the fabrication of ceramic coatings, monoliths, composites, laminates and functionally graded materials varying in thickness from a few nanometres to centimetres.¹ Although the different colloidal processes have in common that ceramic suspensions are used, the requirements for these suspensions differ substantially from one process to another. For processes such as pressure filtration, slip casting and tape casting, a high solids loading up to 40 vol% is required for an acceptable forming rate.² For electrophoretic deposition, the viscosity of the suspensions can be kept low since the solids loading can be much lower (2–10 vol%), while maintaining reasonable forming rates.

Suspension parameters determine the structure and cohesion of the green EPD deposit at the electrode. Stable well-dispersed

suspensions are necessary to produce densely packed deposits.³ The green density should be as high as possible to provide green strength and reduced shrinkage during sintering. Suspension stabilisation can be realised by several mechanisms: by stabilising agents like polyelectrolytes or by surface charging of the powder particles establishing repulsive forces. Because the particles require an electric charge for electrophoresis, EPD literature considers mainly electrostatic stabilisation.

EPD can be performed in aqueous and non-aqueous systems, each of them having advantages and disadvantages. Water is sometimes used as a solvent for electrophoretic deposition, mainly because of environmental and economical reasons. However, due to the electrolysis of water and the concomitant formation of gas bubbles at steel electrodes at voltages above about 3–4 V, the deposit will contain pores due to the gas formation. In the case of plate-shaped components, gas bubbles in the deposit can be prevented by using a membrane in front of the deposition electrode.⁴ For complex shaped components on the other hand, it is not feasible to use a membrane. Another method to avoid gas bubbles is to use palladium electrodes for cathodic EPD from aqueous suspensions. Palladium readily absorbs hydrogen⁵ but is expensive. EPD in non-aqueous suspensions is mostly performed in an alcohol or ketone solvent or a mixture of them. The main advantage of non-aqueous media for EPD is the possibility to use high voltages and consequently, to obtain higher

* Corresponding author. Tel.: +32 16 321244; fax: +32 16 321992.
E-mail address: Jozef.Vleugels@mtm.kuleuven.be (J. Vleugels).

deposition rates. Disadvantages are the toxicity of the solvents and the higher cost. Recuperation of the solvents however can lower the costs and avoid the environmental impact. Some recent articles give an overview of applications and suspension systems for a number of powder materials.^{1,6–9}

Ketone based suspensions with amine additions already proved their applicability for the electrophoretic deposition of Al_2O_3 ,^{10,11} ZrO_2 ,^{10,11} WC-Co ¹² and SiC .¹³ It was shown before that the electrical field strength for MEK + *n*-butylamine based suspensions is constant and no potential drop at the electrodes is observed. This in contrast with ethanol + acid based suspensions where the deposit acts as an extra resistive layer.^{14,15} Therefore, a MEK + *n*-butylamine based suspension is an interesting suspension system for EPD of thick deposits. Despite a good deposition yield, the suspension stability is rather low, which can generate rough surfaces for thick deposits (>5 mm). These suspensions therefore need vigorous stirring, which is not always applicable as for example for the EPD of complex shape components, and the addition of dispersants is essential to improve the stability.

The present work reveals that nitrocellulose is an ideal additive to disperse metal oxide powders in MEK with *n*-butylamine. The effect of nitrocellulose and *n*-butylamine addition on the stability, viscosity and the EPD characteristics of Al_2O_3 - and ZrO_2 based suspensions are investigated as well as the role of the different additives.

2. Experimental procedure

The starting powders are commercially available coprecipitated 3 mol% yttria-stabilised ZrO_2 (Daichi grade HSY-3U) nanopowder and submicrometer sized α - Al_2O_3 (Baikowski grade SM8) powder with a specific surface area of 20 and $10\text{ m}^2/\text{g}$, respectively (supplier data). The as-received Al_2O_3 powder was mixed in ethanol with Y-TZP milling balls (Tosoh grade TZ-3Y) on a multidirectional mixer (type Turbula) for 24 h to break up hard agglomerates. After mixing, the ethanol was evaporated by means of a rotating evaporator and the powder was dried at 90°C . The particle size distribution of the as-received ZrO_2 and milled Al_2O_3 powder, as measured by acoustic particle size analysis (APS-100, MATEC, USA), is shown in Fig. 1.

Suspensions were prepared by suspending 150 g/l of powder in methylethylketone (MEK, Acros, 99%). Subsequently, *n*-butylamine (BA, 99.5%, Acros) and nitrocellulose (NC, Aldrich, 435058-250g) are added. The suspensions are magnetically stirred for 30 min, ultrasonically stirred (Branson 2510 bath) for 15 min, and magnetically stirred again for 30 min.

Electrophoretic deposition at constant voltage (type MCN 1400-50, F.U.G., Germany) is performed with freshly prepared suspensions in an EPD cell consisting of two vertically positioned stainless steel electrodes with a distance of 35 mm. The electrodes have a surface area of 9 cm^2 and the volume of the deposition cell is 50 ml. The edges of the deposition electrode are shielded by a non-conductive cover, made from PTFE.

After deposition, the deposits are dried, weighted and the green density is determined by the Archimedes method using lacquer (Enthone B.V., The Netherlands) encapsulation.

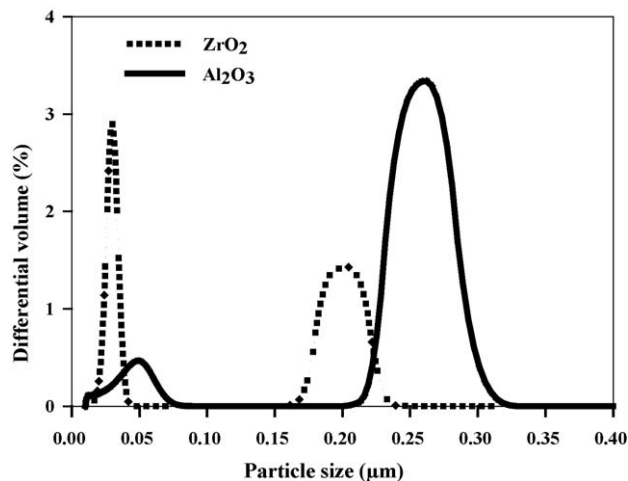


Fig. 1. Particle size distribution of the ZrO_2 and milled Al_2O_3 starting powder, as obtained by acoustic particle size analysis.

Electrophoretic mobility measurements are performed in concentrated suspensions using the electro-acoustic measuring technique (ESA 9800, MATEC, USA). The suspension conductivity was measured with a Cond Level 2 probe (WTW, Germany). The viscosity of some selected suspensions was measured with a capillary viscosity meter (Schott-Geräte GmbH, Germany).

The stability of the suspensions was investigated by measuring the weight change of a cone, suspended at a certain depth in an unstirred suspension as a function of time, using a BP 221S balance (Sartorius, Germany).¹⁴ The slope of the obtained time–weight change curves was calculated over a range of 5000 s. The slope of the suspension without charging additives is used as a reference. This reference slope is divided by the slope obtained for the suspension under investigation in order to determine the stability ratio, *W*, of that specific suspension.

3. Results and discussion

3.1. Suspension stability

The effect of the addition of *n*-butylamine and nitrocellulose on the Al_2O_3 suspension stability is investigated by means of settling rate studies, as shown in Fig. 2. The MEK based suspensions without combined nitrocellulose and *n*-butylamine addition settle very fast. After less than 200 s, almost all powder is settled. Suspensions containing 1 wt.% powder with combined addition of *n*-butylamine and nitrocellulose however only partially settle after 5000 s, indicating that an interaction occurs between the MEK, *n*-butylamine, nitrocellulose and powder particle surface, which is responsible for the stabilisation of the particles in the suspension.

When the mass of nitrocellulose is fixed at 1 wt.% relative to the mass of dry powder, the stability of the alumina suspensions increases with increasing amount of *n*-butylamine, reaching a maximum stability at 10 vol% *n*-butylamine (see Table 1). The stability of the zirconia containing suspensions does not vary as function of the *n*-butylamine content using the same amount of

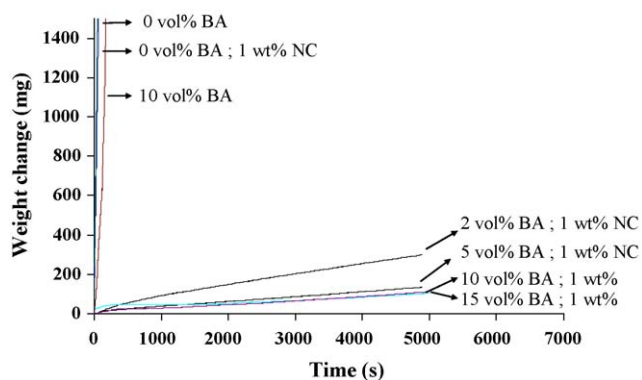


Fig. 2. Stability curves of the Al_2O_3 based suspensions (BA: *n*-butylamine; NC: nitrocellulose).

Table 1

Stability ratio, *W*, for Al_2O_3 and ZrO_2 suspensions based on MEK, BA and nitrocellulose

| <i>n</i> -butylamine (vol%) | Nitrocellulose (wt%) | <i>W</i> (Al_2O_3) | <i>W</i> (ZrO_2) |
|-----------------------------|----------------------|--------------------------------------|-----------------------------|
| 0 | 0 | 1 | 1 |
| 0 | 1 | 1.4 | / |
| 10 | 0 | 2.5 | / |
| 2 | 1 | 410 | 269 |
| 5 | 1 | 891 | 251 |
| 10 | 1 | 1401 | 228 |
| 15 | 1 | 1305 | 235 |

nitrocellulose. The zirconia suspensions are less stable than the alumina suspensions, but the sedimentation rate is still low, as summarised in Table 1.

3.2. Electrophoretic mobility

Electrophoretic mobilities were measured for MEK based Al_2O_3 and ZrO_2 suspensions (100 g/l powder) as a function of the *n*-butylamine content, as presented in Figs. 3 and 4. Because MEK is an electron donor,^{14–17} Y-ZrO_2 and Al_2O_3 powders are negatively charged in MEK. *n*-Butylamine is a stronger base than MEK and the powder particles get more negatively charged

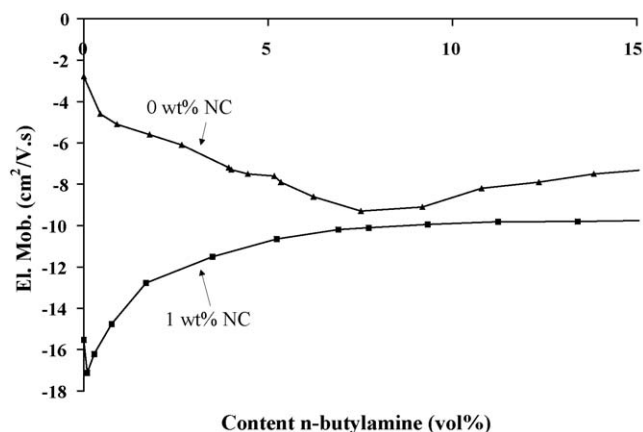


Fig. 3. Electrophoretic mobility of MEK based Al_2O_3 suspensions (100 g/l) as a function of the amount of *n*-butylamine and nitrocellulose.

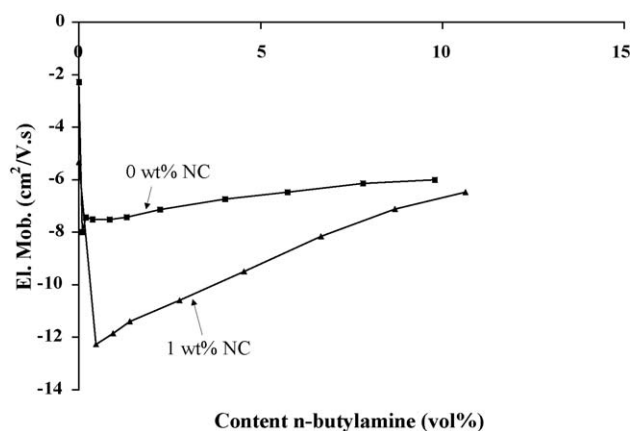


Fig. 4. Electrophoretic mobility of MEK based Y-ZrO_2 suspensions (100 g/l) as a function of the amount of *n*-butylamine and nitrocellulose.

when *n*-butylamine is added to the suspension. In the absence of nitrocellulose, a maximum electrophoretic mobility is reached upon adding 7.5 vol% and 1 vol% of *n*-butylamine for Al_2O_3 and Y-ZrO_2 , respectively. Because of the higher specific surface area of the zirconia powder compared to alumina (see Fig. 1), this difference should be attributed to a higher surface charge density of the alumina powder. When 1 wt% nitrocellulose is added to the suspensions, the electrophoretic mobility increases. Even without butylamine, the addition of nitrocellulose turns the electrophoretic mobility more negative due to the fact that MEK is a weak base and is able to interact with the acidic groups on the adsorbed nitrocellulose. A maximum electrophoretic mobility is reached below 1 vol% butylamine for both powders. The mobility however decreases upon addition of more *n*-butylamine. Although not impossible, it is thought to be unlikely that the nitrocellulose is displaced from the surface by *n*-butylamine, due to the multiple adsorption sites of the nitrocellulose polymer chain. Therefore, the decreased mobility is attributed to the increase in ionic strength. At higher *n*-butylamine concentrations, the electrophoretic mobility is strongly influenced by the ionic strength of the suspension. The absolute value for the electrophoretic mobility is lower for Y-ZrO_2 than for Al_2O_3 . Because the electrophoretic mobility and the concomitant zeta potential reach their maximum at the same amount of *n*-butylamine when nitrocellulose is present, one can assume that the nitrocellulose is adsorbed on the powder surface. The maximum electrophoretic mobility however does not correlate with the highest suspension stability (see Table 1). The zeta potential is normally directly related to the suspension stability, which is not the case for these suspension systems. This means that the zeta potential is probably not the key parameter, which determines the stability of the described alumina and zirconia suspension systems. Therefore, electrosteric stabilisation by the charged adsorbed nitrocellulose, in combination with electrostatic repulsion, play an important role in this system.

3.3. Electrophoretic deposition experiments (EPD)

Electrophoretic deposition experiments were performed with Al_2O_3 and ZrO_2 suspensions (150 g/l) as a function of the

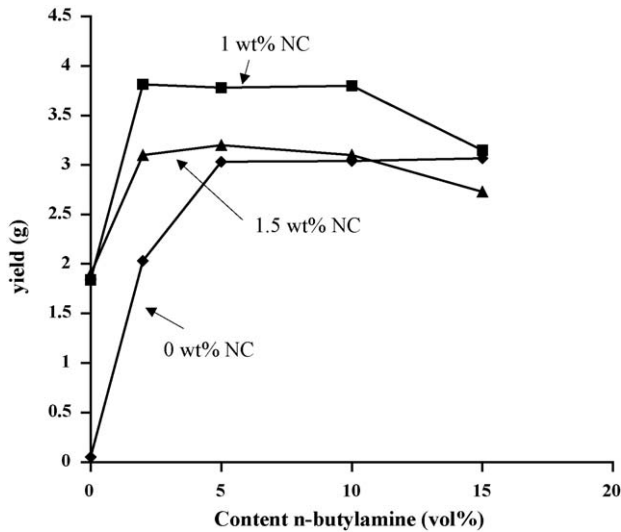


Fig. 5. Al₂O₃ deposition yield after 300 s at 300 V as a function of the amount of *n*-butylamine and nitrocellulose addition.

n-butylamine and nitrocellulose content. The green density and the yield were measured after EPD for 300 s at 300 V. Because the particles are negatively charged, anodic deposition was performed.

With the Al₂O₃ powder, no deposit was obtained from a 100% MEK based suspension. The deposition yield increased with increasing *n*-butylamine content but levels off at 5 vol% *n*-butylamine as shown in Fig. 5. The green density also increases as a function of the *n*-butylamine content from 44% at 2 vol% *n*-butylamine up to 52% at 15 vol% *n*-butylamine, as shown in Fig. 6.

When adding 1 wt.% nitrocellulose to these suspensions, the Al₂O₃ deposition yield increases and reaches a maximum at 2 vol% *n*-butylamine. The green density drastically increases up to 5 vol% *n*-butylamine and is significantly higher than without nitrocellulose addition (see Fig. 6). The addition of 1 wt.%

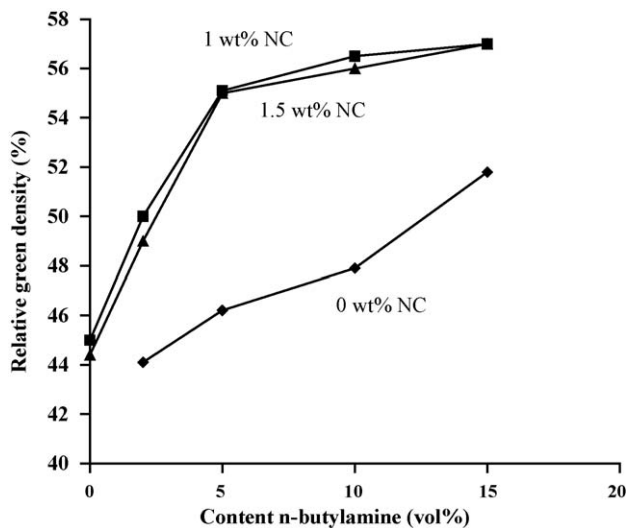


Fig. 6. Al₂O₃ deposit green density after EPD at 300 V for 300 s as a function of the amount of *n*-butylamine and nitrocellulose addition.



Fig. 7. Al₂O₃ deposits obtained from MEK based suspensions containing 1 wt.% nitrocellulose and 2 (left) and 10 (right) vol% *n*-butylamine.

nitrocellulose to MEK without *n*-butylamine gives irregular weak deposits with a low green density of 44%.

When adding 2 vol% *n*-butylamine and 1 wt.% nitrocellulose, Al₂O₃ deposits with a very rough surface are obtained. When the amount of *n*-butylamine is increased, the surface of the deposits becomes very smooth as illustrated in Fig. 7. How the roughness is affected by the suspension stability of the suspension is unclear. But one can assume that convective motion plays an important role.

Increasing the nitrocellulose content from 1 to 1.5 wt.% results in a decreased deposition yield (Fig. 5), whereas the green density of the deposits is the same (Fig. 6). Therefore, 1 wt.% nitrocellulose was used in all further experiments.

At a nitrocellulose content of 1 wt.%, the Al₂O₃ deposition yield decreases with increasing *n*-butylamine content above 2 vol% and becomes almost zero in pure *n*-butylamine (see Fig. 8). The deposition yield correlates well with the decreasing electrophoretic mobility at higher *n*-butylamine contents, as shown in Fig. 3. The green density increases as a function of the *n*-butylamine content at 1 wt.% nitrocellulose addition up to a maximum at 25 vol% *n*-butylamine, whereas the stability ratio increases from 1.4 at 0 vol% *n*-butylamine up to 1305 at 15 vol% *n*-butylamine showing a maximum at 10 vol% butylamine (see Table 1).

For MEK based suspensions with 1 wt.% nitrocellulose, the deposition yield of ZrO₂ follows the same trend as for the Al₂O₃

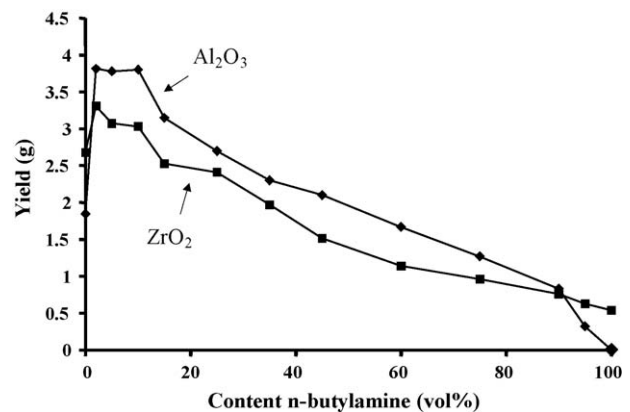


Fig. 8. Al₂O₃ and ZrO₂ deposition yield after 300 s at 300 V from a MEK based suspension with nitrocellulose (1 wt.%) as a function of *n*-butylamine addition.

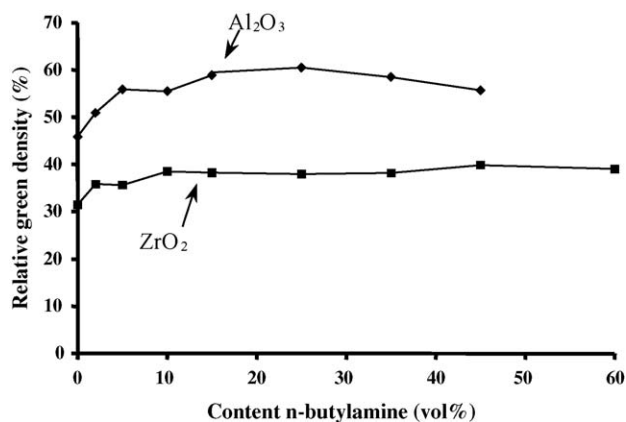
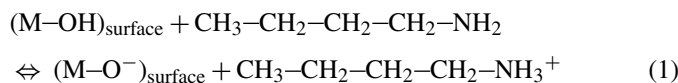


Fig. 9. Green density of Al₂O₃ and ZrO₂ deposits obtained from MEK with 1 wt.% nitrocellulose based suspensions after 300 s at 300 V, as function of the *n*-butylamine content.

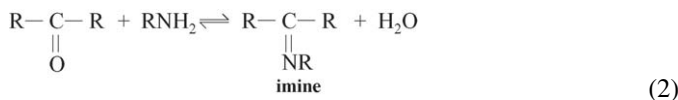
powder. The deposition yield and electrophoretic mobility reach a maximum at 2 vol% *n*-butylamine, as shown in Figs. 4 and 8, whereas the stability of the suspensions remains constant at butylamine contents from 2 to 15 vol% (Table 1). The green density also remains constant at 37%, as shown in Fig. 9. The difference in green density for Al₂O₃ and ZrO₂ (Fig. 9) can be attributed to the significantly smaller particle size distribution of the ZrO₂ powder.

3.4. Role of the different chemicals

The adsorption of *n*-butylamine on an oxide surface is a well-known and studied subject.^{16–19} Since *n*-butylamine is an electron donor, the protons of the surface hydroxyl groups of the metal oxide are transferred to the basic nitrogen atoms of the adsorbed amine molecules:



Besides an acid–base reaction (1), a primary amine such as *n*-butylamine reacts with a ketone (MEK) towards an imine and water²⁰ according to:



The formed imines can be determined qualitatively by infrared spectroscopy.²⁰ The reaction is an equilibrium reaction and can be visualised by the evolution of the conductivity and temperature as a function of time. During the first 1400 s after addition of *n*-butylamine to MEK, the conductivity increases fast. Afterwards, the reaction rate is reduced but slowly continues as shown in Fig. 10. This ongoing reaction is attributed to the polymerisation of the formed imine, which is responsible for the increase in viscosity (Fig. 11) of the solvent mixture as a function of time.

The amount of reaction products of reaction (2) is a function of both the relative amount of *n*-butylamine and MEK and of time. By means of FTIR measurements (Thermo Nicolet Avatar 360), the amount of formed water can be determined.

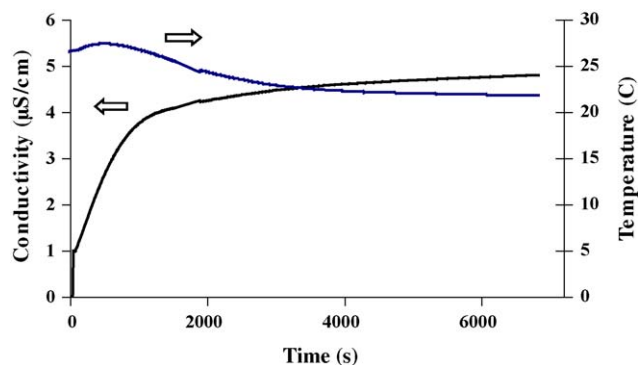


Fig. 10. Evolution of conductivity and temperature as a function of time after addition of 10 vol% butylamine to MEK.

A water–BA calibration curve allowed to establish the following linear relationship between the vol% water and the water peak area between 3300 and 3700 cm⁻¹ in the water–butylamine mixture:

$$Y(\text{vol\% water}) = 1.3676 (\text{peak area water}) \quad (0-20 \text{ vol\% water}) \quad (3)$$

This relationship was used to measure the amount of water in the MEK–BA mixtures without powder addition after 45 min of mixing. This time period was chosen since the conductivity measurements (Fig. 10) indicated that the ketone–amine reaction reached an equilibrium after this time period. The symmetric and asymmetric N–H stretching IR peaks of the amine between 3250 and 3400 cm⁻¹ are not detected in the MEK + 10 vol% *n*-butylamine mixture, as shown in Fig. 12, revealing that reaction (2) completely shifted to the right hand side. Using Eq. (3), the water content in a MEK–*n*-butylamine (90/10) (vol%) was calculated to be about 3 vol%. When the amine content was increased to 20 vol%, the water content in the final mixture after 45 min reaction increased to a maximum of about 4 vol% and the presence of some free amine was detected as shown in Fig. 13. Increasing the *n*-butylamine content above 20 vol% results in a decreasing water content in the final mixture whereas the free *n*-butylamine content increased. Reaction (2) therefore reaches

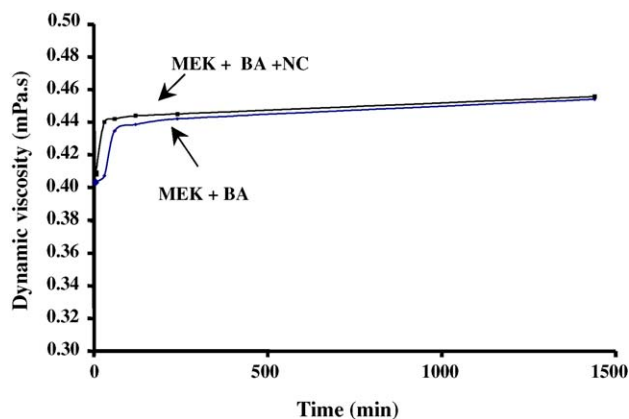


Fig. 11. Evolution of the dynamic viscosity as a function of time after preparation of a solvent mixture of MEK with 10 vol% *n*-butylamine, with and without 1 wt.% nitrocellulose at 23 °C.

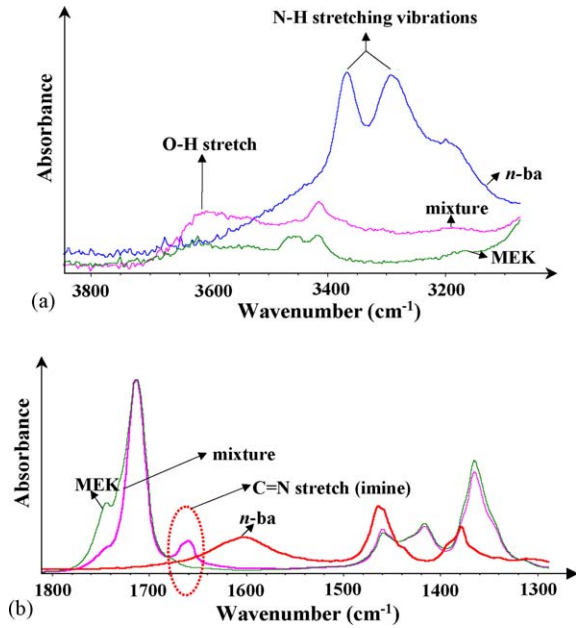


Fig. 12. Details of the FTIR-spectra of methylethylketone (MEK), *n*-butylamine (*n*-BA) and a MEK-butylamine (90/10) mixture. Note the disappearance of the N–H stretching vibrations (a) and the appearance of the C=N stretching vibration (b) when *n*-butylamine is added to MEK.

equilibrium at around 20 vol% butylamine addition with the formation of about 4 vol% H₂O. At higher butylamine additions, the reverse reaction involving the imine will consume a small amount of water, resulting in an overall decreasing H₂O content with increasing butylamine addition above 20 vol%.

Due to the H₂O formation, the electrical conductivity of the suspension changes. The conductivity of an Al₂O₃ based suspension after 45 min in MEK with 1 wt.% nitrocellulose as function of the *n*-butylamine content is shown in Fig. 14. The change in conductivity correlates with the measured water and the free butylamine content shown in Fig. 13.

The increasing electrical conductivity in the 2–20 vol% *n*-butylamine region, due to an increased ionic strength as a result of the formation of water, also explains the reducing electrophoretic mobility and concomitant deposition yield of the ZrO₂ and Al₂O₃ powder with increasing *n*-butylamine content (see Figs. 3–6).

When nitrocellulose is added to a ketone and a metal oxide powder, the nitrocellulose is adsorbed on the powder.²¹ No

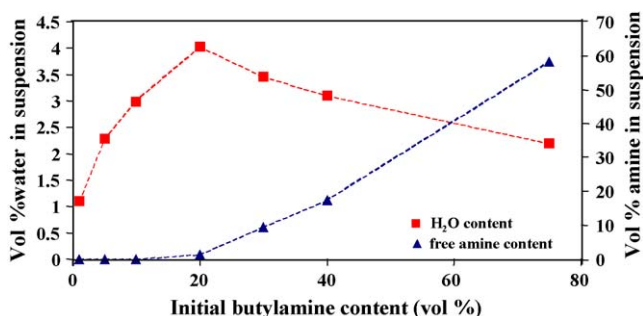


Fig. 13. Calculated amounts of free *n*-butylamine and water (vol%) in MEK–BA mixtures as a function of the initially added amine content (vol%).

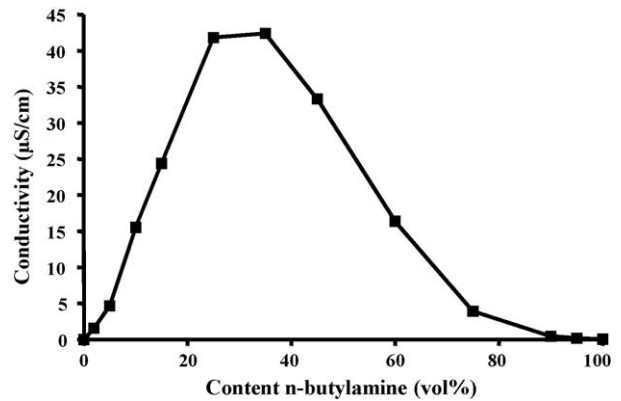


Fig. 14. Conductivity of an Al₂O₃ based suspension after 45 min in MEK with 1 wt.% nitrocellulose as function of the *n*-butylamine content.

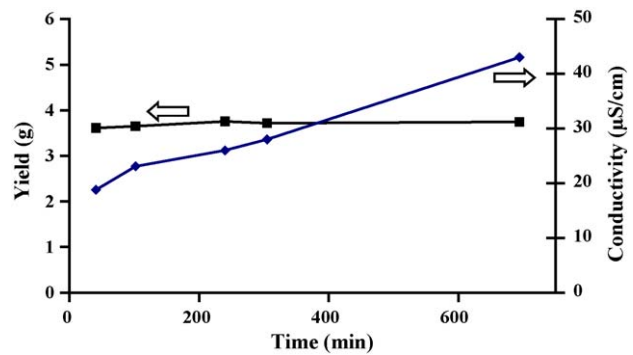


Fig. 15. Conductivity of an Al₂O₃ based suspension in MEK with 10 vol% *n*-butylamine and 1 wt.% nitrocellulose and the deposition yield after 300 s at 300 V as a function of time.

increase in stability of the ZrO₂ and Al₂O₃ particles is observed when only MEK and nitrocellulose are present. The electrophoretic mobility however are drastically increased when a small amount of *n*-butylamine is added to this suspension. The maximum zeta potential is reached upon adding 0.5–1 vol% *n*-butylamine. Therefore, one can assume that a relatively small amount of *n*-butylamine is needed to charge the nitrocellulose, which is adsorbed on the powder particles, leading to electrostatic stabilisation. At higher *n*-butylamine contents, the dissociated water molecules increase the ionic strength and reduce the electrophoretic mobility.

Due to the chemical reaction in the solvent mixture, the electrical conductivity in the suspension increases as function of time, as shown in Fig. 15. However, ageing of the suspension does not influence the EPD behaviour during the first 6 h as illustrated by the constant deposition yield in time (see Fig. 15).

4. Conclusions

Stable suspensions based on methylethylketone (MEK) with combined addition of *n*-butylamine and nitrocellulose were developed for the electrophoretic deposition of Al₂O₃ and ZrO₂ powder. Deposits with a high green density, smooth surface and a high deposition yield were obtained when adding 10–15 vol% *n*-butylamine and 1 wt.% nitrocellulose.

A chemical reaction between the MEK and *n*-butylamine results in the formation of water and imines. The H₂O dissociates and influences the ionic strength of the suspension, whereas the imines polymerise in time. A maximum ZrO₂ and Al₂O₃ electrophoretic mobility is obtained when adding 0.5–1 vol% *n*-butylamine to a 1 wt.% nitrocellulose containing suspension. Due to the formation of water, the ionic strength and electrical conductivity of the suspension increase in the 2–20 vol% *n*-butylamine region, resulting in a reducing electrophoretic mobility and concomitant deposition yield of the ZrO₂ and Al₂O₃ powder with increasing *n*-butylamine content.

The addition of 1 wt.% nitrocellulose to a *n*-butylamine containing MEK suspension resulted in an increased Al₂O₃ and ZrO₂ electrophoretic mobility and a drastically increased green deposit density. The addition of 1.5 wt.% nitrocellulose however reduces the deposition yield. The highest Al₂O₃ suspension stability determined to be at 10–15 vol% *n*-butylamine addition did not coincide with the highest electrophoretic mobility measured at 2 vol% *n*-butylamine, due to the additional electrosteric stabilisation by the adsorbed charged nitrocellulose. This effect was less pronounced for the ZrO₂ powder.

Acknowledgement

This work was supported by the GROWTH program of the Commission of the European Communities under project contract No. G5RD-CT2000-00354, the Fund for Scientific Research Flanders under project No. G.0180.02 and the Research Fund K.U. Leuven under project GOA/2005/08-TBA.

References

1. Van der Biest, O. O. and Vandeperre, L. J., Electrophoretic deposition of materials. *Annu. Rev. Mater. Sci.*, 1999, **29**, 327–352.
2. Lewis, J. A., Colloidal processing of ceramics. *J. Am. Ceram. Soc.*, 2000, **83**(10), 2341–2359.
3. Bouyer, F. and Foissy, A., Electrophoretic deposition of silicon carbide. *J. Am. Ceram. Soc.*, 1999, **82**(8), 2001–2010.
4. Clasen, R. and Tabellion, J., Electric-field-assisted processing of ceramics—Part I: perspectives and applications. *Cfi-Ceram. Forum Int.*, 2003, **80**(10), E40–E45.
5. Uchikoshi, T., Ozawa, K., Hatton, B. and Sakka, Y., Dense, bubble-free ceramic deposits from aqueous suspensions by electrophoretic deposition. *J. Mater. Res.*, 2001, **16**(2), 321–324.
6. Heavens, S., *Electroforetic Deposition as a Processing Route for Ceramics. Advanced Ceramic Processing And Technology*, 7, ed. J. G. P. Binner, 1990, pp. 255–283.
7. Zhitomirsky, I., Cathodic electrodeposition of ceramic and organoceramic materials. Fundamental aspects. *Adv. Colloid. Interf.*, 2002, **97**(1–3), 279–317.
8. Sarkar, P. and Nicholson, P. S., Electrophoretic deposition (EPD): mechanisms, kinetics, and application to ceramics. *J. Am. Ceram. Soc.*, 1996, **79**(8), 1987–2002.
9. Boccaccini, A. R. and Zhitomirsky, I., Application of electrophoretic and electrolytic deposition techniques in ceramics processing. *Curr. Opin. Solid. St. M.*, 2002, **6**(3), 251–260.
10. Put, S., Vleugels, J. and Van der Biest, O., Gradient profile prediction in functionally graded materials processed by electrophoretic deposition. *Acta Mater.*, 2003, **51**(20), 6303–6317.
11. Put, S., Vleugels, J., Anné, G. and Van der Biest, O., Functionally graded ceramic and ceramic-metal composites shaped by electrophoretic deposition. *Coll. Surf. A: Physicochem. Eng. Asp.*, 2003, **222**, 223–232.
12. Put, S., Vleugels, J. and Van Der Biest, O., Functionally graded WC-Co materials produced by electrophoretic deposition. *Script. Mater.*, 2001, **45**(10), 1139–1145.
13. Vandeperre, L. J. and Van Der Biest, O. O., Graceful failure of laminated ceramic tubes produced by electrophoretic deposition. *J. Eur. Ceram. Soc.*, 1998, **18**(13), 1915–1921.
14. Anné, G., Vanmeensel, K., Vleugels, J. and Van der Biest, O., Influence of the suspension composition on the electric field and deposition rate during electrophoretic deposition. *Coll. Surf. A: Physicochem. Eng. Asp.*, 2004, **245**, 35–39.
15. Anné, G., Vanmeensel, K., Vleugels, J. and Van der Biest, O., A mathematical description of the kinetics of the electrophoretic deposition process for Al₂O₃ based suspensions. *J. Am. Ceram. Soc.*, 2005, **88**(8), 2036–2039.
16. Delannay, F., *Characterization of Heterogeneous Catalysts*. Marcel Dekker, Inc., New York and Basel, 1984.
17. Ramis, G. and Busca, G., FT-IR spectra of adsorbed *n*-butylamine. *J. Mol. Struct.*, 1989, **193**, 93–100.
18. Fischer, W. B. and Eysel, H. H., Raman and FTIR spectroscopic study on water structural changes in aqueous solutions of amino acids and related compounds. *J. Mol. Struct.*, 1997, **415**(3), 249–257.
19. Milburn, D. R., Saito, K., Keogh, R. A. and Davis, B. H., Sulfated zirconia: attempt to use *n*-butylamine to measure acidity. *Appl. Catal. A-Gen.*, 2001, **215**(1–2), 191–197.
20. March, J., *Advanced Organic Chemistry: Reactions, Mechanisms and Structure*. L. McGraw-Hill Kogakusha, 1968, pp. 651–726.
21. Mizuguchi, J., Sumi, K. and Muchi, T., A highly stable non-aqueous suspension for the electrophoretic deposition of powdered substances. *J. Electrochem. Soc.*, 1983, **130**(9), 1819–1825.